

New Routes to Synthesizing an Ordered Perovskite $\text{CaCu}_3\text{Fe}_2\text{Sb}_2\text{O}_{12}$ and Its Magnetic Structure by Neutron Powder DiffractionSebastian A. Larregola,[†] Jianshi Zhou,^{*,†} Jose A. Alonso,[‡] Vladimir Pomjakushin,[§] and John B. Goodenough[†][†]Materials Science and Engineering Program, The University of Texas at Austin, Austin, Texas 78712, United States[‡]Instituto de Ciencia de Materiales de Madrid, CSIC, E-28049 Cantoblanco, Madrid, Spain[§]Laboratory for Neutron Scattering, Paul Scherrer Institut, CH-5232 Villigen, Switzerland

Supporting Information

ABSTRACT: The search for new double-perovskite oxides has grown rapidly in recent years because of their interesting physical properties like ferroelectricity, magnetism, and multiferroics. The synthesis of double perovskites, especially the A-site-ordered perovskites, in most cases needs to be made under high pressure, which is a drawback for applying these materials. Here we have demonstrated synthetic routes at ambient pressure by which we have obtained a high-quality duo-sites-ordered double perovskite, $\text{CaCu}_3\text{Fe}_2\text{Sb}_2\text{O}_{12}$, which has been previously synthesized under high pressure. The availability of a large quantity of the powder sample allows us to determine the crystal and magnetic structures by neutron powder diffraction (NPD) at 300 and 1.3 K. Measurements of the magnetization and heat capacity showed a ferrimagnetic transition at 160 K. A ferrimagnetic structure consisting of the uncompensated antiferromagnetic coupling between neighboring collinear copper and iron spins has been resolved from the low-temperature NPD data.

The A-site-ordered perovskite oxides $\text{AA}'_3\text{B}_4\text{O}_{12}$ have been studied extensively because of their wide variety of chemical and physical properties.^{1–3} The A' site in this structure is coordinated by four coplanar oxygen atoms, with short bonds (~2.0 Å) forming nearly square A'O₄ units aligned perpendicularly to each other. Jahn–Teller copper(II) ions are suitable to occupy such a square-coordinated A' site.

Among the many investigated compounds, $\text{Ca}^{2+}\text{Cu}^{2+}_3\text{Ti}^{4+}_4\text{O}_{12}$ ⁴ and $\text{Ca}^{2+}\text{Cu}^{2+}_3\text{Ru}^{4+}_4\text{O}_{12}$ ⁵ are the only known A-site-ordered perovskites that can be prepared at ambient pressures. The stabilization of copper at the A' sublattice (square planar coordination) in all the other cases (for instance, $\text{CaCu}_3\text{Mn}_4\text{O}_{12}$) needs high-pressure and high-temperature conditions, which make them unavailable for many research groups.

Further inclusion of B-site ordering has been achieved in a pair of M^{3+} and M^{5+} at the B site with the general formula $\text{AA}'_3\text{B}_2\text{B}'_2\text{O}_{12}$. These compounds show cationic orderings at the A and B sublattices, having an ordered structure in the B sublattice similar to that observed for $\text{A}_2\text{B}'\text{B}''\text{O}_6$ double perovskites.⁶ As far as we know, seven compounds with this formula have been reported: $\text{CaCu}_3\text{Cr}_2\text{B}_2\text{O}_{12}$ (B = Sb and Ru)^{7,8}

and $\text{CaCu}_3\text{Ga}_2\text{B}_2\text{O}_{12}$ (B = Sb, Nb, Ta, and Ru).^{9,10} All of them needed to be synthesized under pressures and temperatures higher than 11 GPa and 1300 K.

While developing new synthetic routes to obtain A- and B-site-ordered perovskites, we became aware of a study about a new member in this perovskite family, $\text{CaCu}_3\text{Fe}_2\text{Sb}_2\text{O}_{12}$, synthesized under high pressure and high temperature as reported by Chen et al.¹¹ The authors found a ferrimagnetic ordering probably due to a strong $\text{Cu}^{2+}(\uparrow)–\text{Fe}^{3+}(\downarrow)$ antiferromagnetic (AFM) interaction, relieving the predictable frustration between the iron atoms located at the vertices of a regular tetrahedron. A few years before the work of high-pressure synthesis, Xiang et al.¹² calculated the thermodynamics of $\text{CaCu}_3\text{Fe}_2\text{Sb}_2\text{O}_{12}$ by using the generalized gradient approximation (GGA) and GGA+*U* methods. Their calculation predicted that the perovskite $\text{CaCu}_3\text{Fe}_2\text{Sb}_2\text{O}_{12}$ phase would become stable only above 18 GPa. They also predicted a ferrimagnetic semiconducting behavior with a total magnetic moment of 6.17 μ_B per unit cell due to AFM interaction between neighboring copper and iron spins.

In the present study, we have found two alternative ambient-pressure synthesis routes to preparing $\text{CaCu}_3\text{Fe}_2\text{Sb}_2\text{O}_{12}$. Synthesizing the material has been tried by using a conventional solid-state procedure from the mixture and calcination of the oxides, but no pure phase was obtained (the purity is less than 30%). Access at ambient pressure to $\text{CaCu}_3\text{Fe}_2\text{Sb}_2\text{O}_{12}$ required the preparation of very reactive precursors. We prepared the precursors by a wet-chemistry procedure. A mixture of CuO, $\text{Fe}(\text{NO}_3)_3 \cdot 9\text{H}_2\text{O}$, $\text{Ca}(\text{NO}_3)_2$, and Sb_2O_3 oxide was dissolved in a citric acid aqueous solution with some droplets of HNO_3 ; the solution was slowly evaporated at 80 °C, and the resulting resin was decomposed at temperatures of up to 550 °C. The activated powder was then heated following the temperature program detailed in the Supporting Information (SI), giving a high-purity sample (~92%). Alternatively, a successful route was designed by activating the oxides mixture by a ball-milling process. Stoichiometric amounts of CuO, Fe_2O_3 , Sb_2O_3 , and CaCO_3 were put in the ball-milling machine, and the mixture was activated for 36 h at 500 rpm with WC balls (see details in the SI). After this, the sample was heated subsequently at different temperatures. The amorphous phase recrystallizes during heating; it converts into the perovskite phase (97%) only at *T*

Received: February 26, 2014

Published: April 10, 2014

> 820 °C (see Figure S1 in the SI). In both cases, we observed that the material starts to decompose above 950 °C. All of the characterizations were performed on the sample obtained from the mechanical grinding activation due to its higher purity.

The crystal structure of the material was analyzed by the Rietveld method from room-temperature neutron powder diffraction (NPD) data (see Figure 1a). The crystal structure

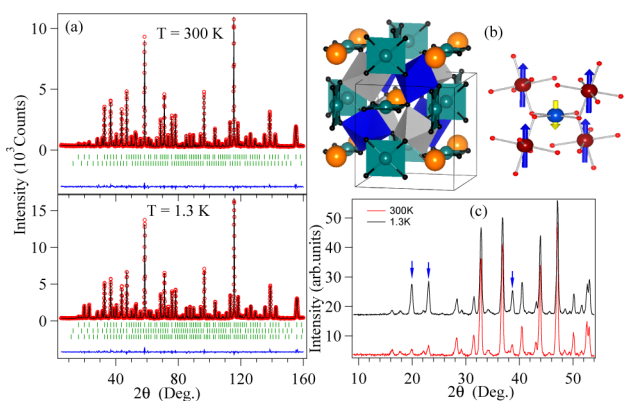


Figure 1. (a) Rietveld refinement of the neutron diffraction patterns at 300 and 1.3 K. The second row of ticks in both refinements corresponds to the Cu₉Sb₄O₁₉ impurity, while the third one in the 1.3 K refinement corresponds to the magnetic structure of the perovskite. (b) Crystal structure and magnetic coupling between the copper magnetic moment (yellow arrow) in CuO₄ polyhedra and the iron ones (blue bigger arrows) at four FeO₆ units. (c) Low-angle region of the 300 and 1.3 K neutron diffraction patterns. The arrows indicate the differences between both patterns.

was refined by using a starting model derived by SPuDs¹³ for AA₃M₂M'₂M''₂O₁₂ perovskites. This compound crystallizes in the *Pn* $\bar{3}$ (No. 201) space group with a unit cell parameter of $\approx 2a_0$, where a_0 is the unit cell parameter of the primary cubic structure of ABO₃ perovskite. Table S1 in the SI shows the main results obtained from the refinement, and a schematic view of the structure is shown at Figure 1b, which is characterized by the presence of heavy in-phase octahedral tilting along the (111) direction of the cubic cell ($a^+a^+a^+$ in Glazer's notation) with $\theta = 20.32^\circ$ and by 100% cationic ordering between iron and antimony, along the same (111) cubic direction. In comparison, the long-range-order parameter S , defined as $S = 2B_{\text{occ}} - 1$, where B_{occ} is the cation occupancy at the B site, is 0.91 for the sample synthesized under high pressure. The synthesis at ambient pressure allows the sample to cool gradually, whereas the quenching method is normally used in the high-pressure synthesis, which would introduce easily some degree of ion disorder. The Fe–O and Sb–O bond lengths are in agreement with those obtained from tabulated ionic radii,¹⁴ and the bond valence sum (BVS) calculations give divalent copper and trivalent iron. Moreover, site-occupancy refinements show no deviation from the nominal CaCu₃Fe₂Sb₂O₁₂ stoichiometry.

The global instability index (GII) calculated with SPuDs has been used to predict the possible formula of ordered perovskites. For those with smaller GII values, such as CaCu₃Ti₄O₁₂ with a GII of 0.003 valence units (vu), the perovskite phase can be obtained under ambient pressure. The GII is the difference between the formal valence and that from the bond valence sum. While the pressure effect on GII is not clear, it has been demonstrated from existing examples^{7–11,15} that a formula with a higher GII value normally requires high-pressure synthesis in

order to stabilize the perovskite phase. A calculation with SPuDs gives a GII of 0.033 vu for CaCu₃Fe₂Sb₂O₁₂. The synthesis of other CaCu₃M₂M'₂O₁₂ with similar GII values or even smaller needs to be performed under high pressure. Although the critical value of GII above which high-pressure synthesis is needed remains unknown, the result presented in this work indicates that stabilization of the ordered perovskites with higher GII values can be made via designed synthetic routes at ambient pressure. This finding is important for the mass production of ordered perovskites with exotic physical properties.

The M versus H curve in Figure 2a was measured at 5 K; it shows ferrimagnetic behavior, and a small magnetic field induces

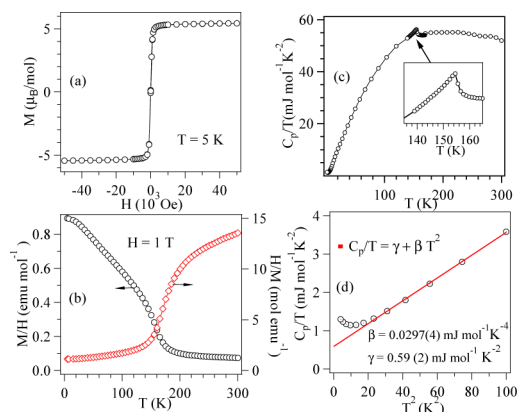


Figure 2. (a) Field dependence of the magnetization. (b) Temperature dependence of the magnetization M/H . The blue line indicates the fit detailed at the figure. (c) Temperature dependence of the heat capacity; Inset: at the transition region. (d) The plot of C_p/T versus T^2 .

sharp saturation of the magnetization with a negligible coercive force. The saturation magnetization value calculated was 5.35 μ_B /formula unit (fu), which is smaller than 7 μ_B /fu, predicted based on a model of an ideal collinear ferrimagnetic coupling between Fe³⁺ ($S = 5/2$) and Cu²⁺ ($S = 1/2$). However, the temperature dependence of magnetic susceptibility $\chi(T)$ in Figure 2b is indeed typical of ferrimagnetic materials with $T_N \sim 160$ K. A linear range cannot be found in $\chi^{-1}(T)$ at $T > T_N$ up to 300 K.

The room-temperature resistance of CaCu₃Fe₂Sb₂O₁₂ was higher than 10⁷ Ω , indicating localized electronic states on the iron and copper ions. Figure 2c shows the temperature dependence of the heat capacity (C_p/T) measured at zero magnetic field between 300 and 1.8 K. Corresponding to the magnetic transition derived from $\chi(T)$, a λ peak is observed at 160 K. Furthermore, the C_p/T versus T^2 plot (Figure 2d) shows linear behavior below 15 K, and extrapolation to $T = 0$ K gave a γ value of 0.57(5) mJ/mol·K². The small deviation of γ from zero (expected value for an insulator) is intriguing and appears to be related to quantum spin fluctuations from the residual spin degree of freedom on Fe³⁺. As shown by the magnetization and neutron diffraction, Fe³⁺ does not show the full moment.

By taking advantage of the large quantity of sample (>5 g) synthesized at ambient pressure, we have carried out high-resolution neutron diffraction on CaCu₃Fe₂Sb₂O₁₂ at 300 and 1.3 K, which allows us to further verify the crystal and magnetic structures proposed previously. Figure 1c shows the low-angle regions of the diffraction patterns at 300 and 1.3 K; some low-angle reflections experience an intensity growth (111, 200, and 311) with a propagation vector $k = 0$ at 1.3 K. The absence of additional reflections (splitting or satellites) suggests that the

crystal structure remains cubic and the magnetic structure is collinear. The refinement for the pattern at 1.3 K with the $Pn\bar{3}$ space group (Figure 1a and Table S1 in the SI) reveals a contraction of the unit cell volume associated with the contraction of the M–O bond lengths. A slight increase of the BVSs of the metallic atoms gives no evidence of a possible intersite charge transfer. The octahedral-site tilting angle increased slightly by 0.075° upon cooling.

The refinement based on a model with copper and iron spins antiparallel along the c axis and resultant magnetic moments of $-0.93(4) \mu_B/\text{Cu}$ and $4.33(4) \mu_B/\text{Fe}$ turns out to be extremely good with the discrepancy factor $R_{\text{Mag}} = 2.01\%$. The moment reduction relative to the theoretical magnetic moments ($S = 1/2$ and $5/2$, respectively) may be partially accounted for by the AF coupling. The net moment from neutron diffraction is $5.87 \mu_B/\text{fu}$, which matches very well that obtained from the magnetization measurement in this work. In comparison, the X-ray magnetic circular dichroism measurement gave a slightly lower moment of $5.41 \mu_B/\text{fu}^{11}$ for the sample synthesized under high pressure, which could be attributed to a relatively large disorder during quenching of the sample.

Xiang et al.¹² performed GGA+ U calculations on a structure with hypothetical bond lengths Cu–O = 1.960 Å and Fe–O = 2.038 Å at 0 K (quite close to that obtained in this work at 1.3 K; see Table S1 in the SI); they have obtained moments of $0.70 \mu_B/\text{Cu}$ and $4.17 \mu_B/\text{Fe}$, and a net moment per unit formula of $6.24 \mu_B$, which is close to the value of the sample made at ambient pressure.

It is interesting to notice that the spins at the Fe^{3+} ions are not pointing to either a corner oxygen or an edge or a face of FeO_6 octahedra but are oriented strictly along the c axis. As in other A-site-ordered perovskites (for example, $\text{CaCu}_3\text{Ir}_4\text{O}_{12}$ ¹⁶), the t_2 orbital within the CuO_4 plane is half-filled.¹² Therefore, the superexchange interaction via Cu–O–Fe is AFM. The strong single-ion anisotropy at Cu^{2+} with coplanar coordination locks the spin either normal to the plane or within the plane perfectly. The AFM coupling between Cu^{2+} and Fe^{3+} aligns the moment on iron.

In conclusion, the neutron diffraction study reveals that the $Pn\bar{3}$ phase of the duo-site-ordered perovskite $\text{CaCu}_3\text{Fe}_2\text{Sb}_2\text{O}_{12}$ remains stable down to 1.3 K, and the temperature dependence of the atomic positions appears to be extremely small. The structural study has also verified the model of collinear, antiparallel spins on Cu^{2+} and Fe^{3+} . Most importantly, instead of using high-pressure synthesis, we have demonstrated the possibility of stabilizing these double perovskites with a high GII value at ambient pressure. The GII and geometric tolerance factor t are basic parameters in the design of new double perovskites. However, the constraint from the GII consideration can be avoided in synthesizing $\text{CaCu}_3\text{Fe}_2\text{Sb}_2\text{O}_{12}$. Whether the synthesis of $\text{CaCu}_3\text{Fe}_2\text{Sb}_2\text{O}_{12}$ at ambient pressure is a peculiar case or a modified definition of GII is needed in order to truly reflect the structural instability requires further study.

■ ASSOCIATED CONTENT

📄 Supporting Information

Sample synthesis, structural refinement and the results, and procedures for measuring the physical properties. This material is available free of charge via the Internet at <http://pubs.acs.org>.

■ AUTHOR INFORMATION

Corresponding Author

*E-mail: jszhou@mail.utexas.edu.

Notes

The authors declare no competing financial interest.

■ ACKNOWLEDGMENTS

This work was supported by NSF DMR 1122603 and the Welch foundation(F-1066).

■ REFERENCES

- (1) Shimakawa, Y. *Inorg. Chem.* **2008**, *47*, 8562–8570.
- (2) Shimakawa, Y.; Saito, T. *Phys. Status Solidi* **2012**, *B* 249 (No. 3), 423–434.
- (3) Long, Y. W.; Hayashi, N.; Saito, T.; Azuma, M.; Muranaka, S.; Shimakawa, Y. *Nature* **2009**, *458*, 60–63.
- (4) Subramanian, M. A.; Li, D.; Duan, N.; Reisner, B. A.; Sleight, A. W. *J. Solid State Chem.* **2000**, *151*, 323–325.
- (5) Kobayashi, W.; Terasaki, I.; Takeya, J.-I.; Tsukada, I.; Ando, Y. *J. Phys. Soc. Jpn.* **2004**, *73*, 2373–2376.
- (6) Galasso, F.; Katz, L.; Ward, R. *J. Am. Chem. Soc.* **1959**, *81*, 820–823.
- (7) Byeon, S.-H.; Lee, S.-S.; Parise, J. B.; Woodward, P. M.; Hur, N. H. *Chem. Mater.* **2005**, *17*, 3552–3557.
- (8) Byeon, S.-H.; Lee, S.-S.; Parise, J. B.; Woodward, P. M. *Chem. Mater.* **2006**, *18*, 3873–3877.
- (9) Byeon, S.-H.; Lufaso, M. W.; Parise, J. B.; Woodward, P. M.; Hansen, T. *Chem. Mater.* **2003**, *15*, 3798–3804.
- (10) Byeon, S.-H.; Lee, S.-S.; Parise, J. B.; Woodward, P. M.; Hur, N. H. *Chem. Mater.* **2004**, *16*, 3697–3701.
- (11) Chen, W.-t.; Mizumaki, M.; Saito, T.; Shimakawa, Y. *Dalton Trans.* **2013**, *42*, 10116–10120.
- (12) Xiang, H.; Wang, J.; Meng, J.; Wu, Z. *Comput. Mater. Sci.* **2009**, *46*, 307–309.
- (13) Lufaso, M. W.; Woodward, P. M. *Acta Crystallogr., Sect. B* **2001**, *57*, 725–738.
- (14) Shannon, R. D. *Acta Crystallogr., Sect. A* **1976**, *32*, 751–767.
- (15) Lufaso, M. W. Ph.D. Thesis, The Ohio State University, Columbus, OH, 2002.
- (16) Cheng, J.-G.; Zhou, J.-S.; Yang, Y.-F.; Zhou, H. D.; Matsubayashi, K.; Uwatoko, Y.; MacDonald, A.; MacDonough, J. B. *Phys. Rev. Lett.* **2013**, *111*, 176403_1–176403_5.